TELKOMNIKA Telecommunication, Computing, Electronics and Control
Vol. 24, No. 5, October 2026, pp. 1699∼1709
ISSN: 1693-6930, DOI: 10.12928/TELKOMNIKA.v24i5.27784

Robustness analysis of distributed CFAR detection with K-out-of-L fusion in heterogeneous environments

Pham Van Hung, Nguyen Dinh Tinh
Department of Radar, Faculty of Radio-Electronic Engineering, Le Quy Don Technical University, Hanoi, Vietnam

Article Info

Article history:

Received Jan 7, 2026
Revised Apr 27, 2026
Accepted May 25, 2026

Keywords:

Constant false alarm rate processors
Distributed detection
Non-homogeneous environments
Order statistics constant false alarm rate
Poisson binomial distribution

ABSTRACT

To operate effectively in complex environments, distributed radar systems require a robust constant false alarm rate (CFAR) processor. Conventional distributed cell-averaging (D-CA) CFAR detectors are optimal in homogeneous noise. However, they suffer severe performance degradation in non-homogeneous scenarios, specifically under multiple interfering targets and abrupt clutter edges. This study presents a comprehensive performance analysis of distributed order statistics (D-OS) CFAR systems employing the K-out-of-L fusion rule. We derive the exact global detection and false alarm probabilities using the Poisson binomial distribution. These models are implemented via variable precision arithmetic to ensure numerical stability under extreme masking conditions. Detection thresholds are rigorously calibrated to maintain a fixed global false alarm rate of 10^{-4} in homogeneous backgrounds. Quantitative results demonstrate that D-OS-CFAR significantly outperforms the D-CA-CFAR baseline. It maintains stable detection performance ($P_D > 0.9$) under clutter power variation and suppresses false alarm surges at clutter edges to approximately 4.5×10^{-4}. The analysis concludes that lower-K rules (e.g., $K = 1, 2$) offer the optimal trade-off, limiting the homogeneous CFAR loss to below 0.5 dB while ensuring stable operation in highly heterogeneous environments.

Corresponding Author:

Nguyen Dinh Tinh
Department of Radar, Faculty of Radio-Electronic Engineering, Le Quy Don Technical University
236 Hoang Quoc Viet, Hanoi, Vietnam
Email: tinhnd_k31@lqdtu.edu.vn

1. INTRODUCTION

The capability to automatically detect targets in non-stationary noise and clutter environments is a fundamental requirement for modern surveillance systems, ranging from radar networks to distributed wireless sensor networks (WSN) and internet of things (IoT) applications [1]-[5]. In these decentralized architectures, maintaining a predictable performance level is critical. Constant false alarm rate (CFAR) processors [6], [7] are widely employed to adaptively set the detection threshold based on local estimates of the background interference.

The conventional cell-averaging CFAR (CA-CFAR) detector, first proposed by Finn and Johnson [8], is the optimum processor under the assumption of a homogeneous background with exponential distribution. However, in realistic operational scenarios, the background environment is rarely homogeneous. The performance of CA-CFAR severely degrades in non-homogeneous environments, specifically in the presence of multiple interfering targets or abrupt clutter edges [9], [10]. In multiple-target situations, the averaging logic causes the threshold to rise unnecessarily, leading to detection losses that can exceed 10–20 dB (the "masking effect"), causing the primary target to be missed. Conversely, at clutter edges, the inclusion of high-power clutter samples in the estimation window can cause the false alarm probability to surge uncontrollably, often increasing by orders of magnitude (e.g., from 10^{-4} to 10^{-1}), thereby saturating the fusion center (FC) with false tracks [6], [7]. To mitigate these performance losses, robust CFAR techniques based on order statistics (OS) have been developed [11]. By selecting the k-th rank-ordered sample as the noise estimate, the OS CFAR can effectively reject up to $N - k$ interfering pulses, exhibiting superior robustness compared to mean-level detectors [12]-[14]. While various complex local variants have recently emerged to enhance single-sensor adaptability [15]-[22], the challenge shifts to maintaining this robustness across decentralized networks.

Parallel to the advancements in local processing, distributed detection has garnered significant attention. In a decentralized architecture with decision fusion, local sensors transmit compressed decisions (typically 1-bit) to a FC, which combines them according to a specific rule [23]. Barkat and Varshney [24] analyzed the performance of distributed CA-CFAR (D-CA-CFAR) using "AND" and "OR" rules. However, similar to the single-sensor case, D-CA-CFAR remains vulnerable to non-homogeneous clutter. Recognizing this limitation, Uner and Varshney [25] extended the analysis to distributed OS-CFAR (D-OS-CFAR), demonstrating its superiority in multi-target scenarios. Subsequent studies have focused on optimizing parameters [26]-[28], considering statistical dependence [29], [30], or modeling non-Gaussian clutter [31]-[33].

Despite this solid foundation, a critical research gap remains: the existing literature predominantly restricts analytical models to simplified configurations (e.g., two-sensor systems or simple "AND/OR" logic) and often overlooks numerical instability in extreme interference. To bridge this gap, the novelty of this study lies in analyzing the exact robustness of the generalized K-out-of-L fusion rule under non-homogeneous clutter conditions and precisely quantifying its performance degradation. This study is among the first to derive exact closed-form global detection and false alarm probabilities for D-OS-CFAR under the generalized K-out-of-L fusion rule.

Accordingly, the major contributions of this work are as follows: (i) we formulate exact closed-form expressions for the global probability of detection (P_D) and false alarm (P_F) in non-homogeneous environments using the Poisson binomial distribution [34], generalizing the analysis for any network size L and voting rule K; (ii) we implement a variable precision arithmetic (VPA) approach [35] to eliminate catastrophic cancelation errors [36], establishing a precise numerical benchmark for extreme masking scenarios often missed by standard approximations; and (iii) we provide a comprehensive quantitative analysis, assessing the system's immunity to high-power interfering targets and its capability to suppress false alarm surges at clutter edges. These findings provide critical design guidelines for implementing reliable distributed detection frameworks in heterogeneous environments, which are applicable to both radar systems and cognitive sensor networks.

The rest of the outline for the paper is below. Section 2 describes the proposed system model. Section 3 presents the methodology of performance analysis, including closed-form expressions. Section 4 presents the numerical results. Finally, section 5 concludes the paper with key findings, limitations, and future work.

2. SYSTEM MODEL

Consider a decentralized detection system consisting of L distributed radar sensors and a FC, as shown in Figure 1. Each radar sensor receives echoes from the target–environment scene and performs a processing chain comprising the radio frequency (RF) / antenna front-end, local signal processing, and a CFAR detector that produces a local decision u_i ($i = 1, \ldots, L$). These local decisions are transmitted to a FC, where the global decision U is obtained by applying logical fusion rules (AND, OR, K-out-of-L). This distributed structure exploits the spatial diversity of multiple sensors to enhance the probability of detection at a given false-alarm rate while preserving the overall system's modularity and scalability. We assume a symmetric system configuration in which all local detectors share identical parameters (reference window size N, order number k, and threshold multiplier T).

2.1. Local CFAR detector model

Figure 2 depicts the CFAR detection mechanism employed at each sensor. A sliding CFAR window extracts the reference cells around the cell under test (CUT), and the CFAR logic (e.g., CA or OS) forms the clutter estimate. The output samples in the reference window, denoted by $X_1, X_2, \ldots, X_N$, and the sample in CUT, denoted by Y_i, follow an exponential distribution with the following probability density function:

$$f(x) = \frac{1}{\lambda} \exp\left(-\frac{x}{\lambda}\right), \quad x \geq 0 \tag{1}$$

where λ represents the sample's average power.

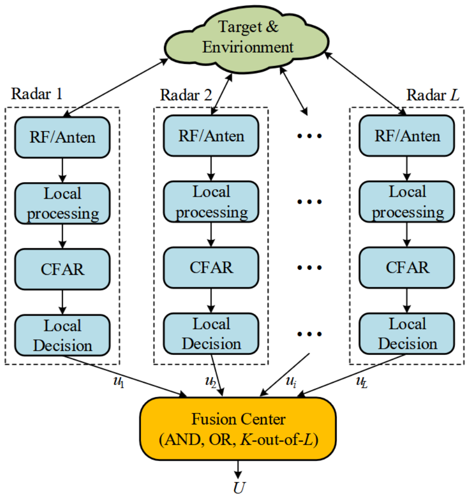

Figure 1. The distributed detection system

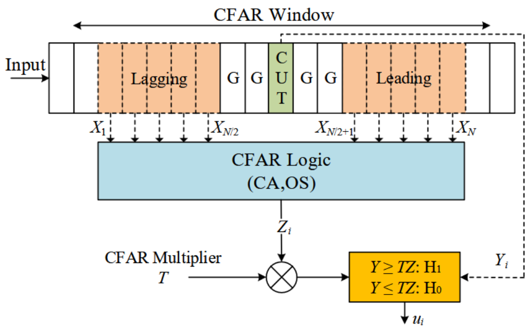

Figure 2. A local CFAR processing

The following binary hypothesis testing problem is considered:
- Hypothesis H_0: the CUT contains only thermal noise (or a clutter background). The average power is $\lambda = \mu$.
- Hypothesis H_1: the CUT contains a target plus noise. The average power is $\lambda = \mu(1 + S)$, where S is the average signal-to-noise ratio (SNR) of the primary target. We assume a slowly fluctuating Swerling I target model.

Each local sensor i ($i = 1, \ldots, L$) estimates the noise power Z_i from the reference window using a CFAR processor. The local decision u_i is made as (2):

$$u_i = \begin{cases} 1, & \text{if } Y_i > TZ_i \\ 0, & \text{otherwise} \end{cases} \tag{2}$$

where T is the scaling factor used to set the desired false alarm rate.

In this study, we analyze two CFAR schemes:
- CA-CFAR: the noise estimate is the sum of the reference samples $Z = \sum_{j=1}^{N} X_j$.
- OS-CFAR: the reference samples are ranked $X_{(1)} \leq X_{(2)} \leq \cdots \leq X_{(N)}$, and the k-th sample is selected as the estimate, $Z = X_{(k)}$.

2.2. Fusion rule

Local binary decisions u_i are transmitted over error-free channels to the FC. The FC employs the generalized "K-out-of-L" voting rule to make the global decision U_0. Specifically, the global decision declares target presence if at least K out of L local detectors report detection:

$$U_0 = \begin{cases} 1, & \text{if } \sum_{i=1}^{L} u_i \geq K \\ 0, & \text{otherwise} \end{cases} \tag{3}$$

where K is an integer ($1 \leq K \leq L$). Note that the logical "OR" rule corresponds to $K = 1$, and the "AND" rule corresponds to $K = L$.

2.3. Non-homogeneous environment models

To evaluate the system's robustness, we define two distinct non-homogeneous scenarios affecting the local sensors. Throughout this analysis, the background interference is assumed to follow an exponential distribution (corresponding to a Rayleigh envelope), and the heterogeneity is modeled as an abrupt variation in the average power level:

- Multiple interfering targets: in this scenario, m cells within the reference window of a "interfered" sensor contain high-power interfering targets with average power $\mu(1+I)$, where I is the interference-to-noise ratio (INR). The remaining $N-m$ cells contain thermal noise μ.
- Clutter edge: this scenario models the radar beam's transition across a background power discontinuity. The reference window contains q cells from a clutter region with power $\mu(1+C)$, where C is the clutter-to-noise ratio (CNR), and $N-q$ cells from the clear region with power μ. The CUT may reside in either the clear region (CUT in noise) or the clutter region (CUT in clutter).

3. PERFORMANCE ANALYSIS

In this section, the exact expressions for the global probability of false alarm (P_F) and detection (P_D) are derived. In this study, we use uppercase and lowercase subscripts to differentiate between global and local probabilities, respectively.

3.1. Local detection probabilities

The probability that a local sensor i declares a detection, denoted as $P_i = Pr(u_i = 1)$, depends on the specific CFAR algorithm and the environment.

3.1.1. Homogeneous background

When the environment is homogeneous ($m = 0$ or $q = 0$), the local false alarm (P_f) and detection (P_d) probabilities for OS-CFAR are given by [11]:

$$P_f = \prod_{j=0}^{k-1} \frac{N-j}{N-j+T}, \quad P_d = \prod_{j=0}^{k-1} \frac{N-j}{N-j+\frac{T}{1+S}} \tag{4}$$

For CA-CFAR, the expressions are [8]:

$$P_f = (1+T)^{-N}, \quad P_d = \left(1+\frac{T}{1+S}\right)^{-N} \tag{5}$$

3.1.2. Non-homogeneous background

The reference window samples are no longer identically distributed for the non-homogeneous scenarios defined in section 2.3. We adopt the general analytical form derived by Gandhi and Kassam [10]. For an OS-CFAR detector where the reference window contains two groups of samples (group 1 with size N_1, power μ_1 and group 2 with size N_2, power μ_2), the probability that the CUT (with power μ_Y) exceeds the threshold $TX_{(k)}$ is as (6):

$$P(Y > TX_{(k)}) = \sum_{i=k}^{N} \sum_{j=\max(0,i-N_2)}^{\min(i,N_1)} \binom{N_1}{j}\binom{N_2}{i-j} \times \mathcal{A}(i,j) \tag{6}$$

where the term $\mathcal{A}(i,j)$ is defined as (7):

$$\mathcal{A}(i,j) = \sum_{a=0}^{j}\sum_{b=0}^{i-j} \binom{j}{a}\binom{i-j}{b}(-1)^{a+b}\left[1+\frac{\mu_Y}{T}\left(\frac{a+N_1-j}{\mu_1}+\frac{b+N_2-(i-j)}{\mu_2}\right)\right]^{-1} \tag{7}$$

The term $\mathcal{A}(i,j)$ encapsulates the complex summation of probability densities resulting from the OS operation on non-identically distributed samples. This accounts for all possible permutations where j interfering samples and $i-j$ noise samples fall below the rank k, ensuring the exact evaluation of the local detection probability without approximation. This general formula is applied as:
- Interfering targets: $N_1 = N-m, \mu_1 = \mu$; $N_2 = m, \mu_2 = \mu(1+I)$
- Clutter edge: $N_1 = N-q, \mu_1 = \mu$; $N_2 = q, \mu_2 = \mu(1+C)$

For CA-CFAR in non-homogeneous backgrounds, we use the moment generating function approach as detailed in [25].

3.1.3. Numerical stability

In strong masking scenarios (e.g., $I \gg 1$ or $C \gg 1$), the local probabilities can become extremely small (e.g., $< 10^{-15}$). Standard double-precision arithmetic often suffers from catastrophic cancelation in the alternating sums of $\mathcal{A}(i, j)$, leading to erroneous negative probabilities [36]. To address this issue, we implemented VPA using the MATLAB Symbolic Math Toolbox [35] to ensure exact evaluation. This information is particularly useful and reliable for the observations in section 4.4 of this paper.

It is important to acknowledge that the implementation of VPA incurs a significantly higher computational cost compared to standard double-precision arithmetic. In this study, VPA is strictly utilized as an offline numerical benchmark to ensure the rigorous validation of the theoretical derivations at these extreme tails. From a practical implementation perspective, real-time distributed radar systems would not perform VPA calculations online. Instead, the exact expressions derived here should be used to generate accurate pre-computed look-up tables or threshold maps. This approach combines the precision of the exact analytical model with the low-latency requirements of the operational hardware.

3.2. Global performance using poisson binomial distribution

To evaluate the overall system performance, it is necessary to establish how local detection probabilities mathematically propagate to the global decision level. Consider a network where p sensors are located in a non-homogeneous environment (e.g., affected by interference) and $L - p$ sensors remain in a homogeneous background. Local detection probabilities are no longer identical across the network. In such cases, the total number of local detections follows the Poisson Binomial distribution, which models the number of successes in independent but non-identically distributed Bernoulli trials [36]. Let P_{inter} and P_{clean} denote the detection probabilities of the interfered and unaffected sensors, respectively.

Since the sensors within each respective group share identical local probabilities, the discrete random variables j and i follow independent Binomial distributions:

- For the interfered group: $P(j) = \binom{p}{j} P_{inter}^{j} (1 - P_{inter})^{p-j}$, where $0 \leq j \leq p$.
- For the clean group: $P(i) = \binom{L-p}{i} P_{clean}^{i} (1 - P_{clean})^{L-p-i}$, where $0 \leq i \leq L - p$.

Because the two groups operate independently, the joint probability of obtaining exactly j interfered detections and i clean detections is simply the product of their individual probabilities.

At the FC, the generalized K-out-of-L rule dictates that a global detection is declared if the total number of local detections $(i + j)$ is greater than or equal to K. To elegantly capture all valid combinatorial pairs of (i, j) that satisfy this condition without utilizing complex summation boundaries, we introduce the indicator function $\mathbb{I}(i + j \geq K)$, which equals 1 if the condition is met and 0 otherwise. Consequently, the global probability (P_F or P_D for either H_0 or H_1) can be derived by summing the joint probabilities over all possible values of i and j, filtered by the indicator function. This yields the following closed-form expression:

$$P_{F,D} = \sum_{i=0}^{L-p} \sum_{j=0}^{p} \mathbb{I}(i + j \geq K) \binom{L-p}{i} P_{clean}^{i} (1 - P_{clean})^{L-p-i} \binom{p}{j} P_{inter}^{j} (1 - P_{inter})^{p-j} \tag{8}$$

This formulation allows for an exact system performance analysis under any arbitrary mix of sensor conditions.

4. NUMERICAL RESULTS AND DISCUSSION

In this section, we present the numerical evaluation of the proposed symmetric D-OS-CFAR system and compare its performance with that of the conventional D-CA-CFAR.

4.1. Simulation setup

To ensure reproducibility, the simulation parameters are defined as:

- Network size: $L = 4$ sensors.
- CFAR window: size $N = 24$, guard cells $G = 0$.
- Order statistic: rank $k = 20$ (providing rejection capacity $N - k = 4$, (approximately $4N/5$)).
- Design probability: global $P_F = 10^{-4}$ in homogeneous background.

To ensure a fair comparison, the threshold parameters (T) for both systems are rigorously calibrated in a homogeneous environment ($p = 0$) to achieve a unified global false alarm probability for every specific fusion rule K ($K = 1, \ldots, L$).

Note that while a network size of $L = 4$ is selected for simulation to clearly visualize the performance differences between specific voting rules (e.g., AND, OR, and majority), the proposed analytical framework is scalable and applicable to any network size L. The computational complexity of the exact derivation scales linearly with L, making it feasible for larger sensor networks. Furthermore, the performance curves presented in the subsequent sections are generated using the exact analytical expressions derived in section 3. As these are theoretical values calculated via VPA, they are free from statistical variance.

4.2. Baseline performance in homogeneous background

Figures 3(a) and 3(b) illustrate the global probability of detection (P_D) versus SNR in a homogeneous environment for D-CA-CFAR (Figure 3(a)) and D-OS-CFAR (Figure 3(b)). Both systems exhibit the standard S-curve behavior, with lower-K rules (e.g., OR rule) yielding higher detection probabilities at the cost of lower thresholds. Furthermore, the 2 out of 4 rule presents the best performance at lower SNR values. As observed in Figure 3, the D-OS-CFAR system requires a slightly higher SNR to achieve the same detection probability as the D-CA-CFAR system. This performance degradation represents the inherent CFAR loss exchanged for the robustness gained in non-homogeneous environments. A quantitative evaluation of the required SNR reveals that the CFAR loss increases marginally at higher detection requirements and varies depending on the specific fusion rule. For instance, to achieve a standard detection probability of $P_D = 0.9$, the D-OS-CFAR system imposes an acceptable CFAR loss ranging from approximately 0.1 dB (for stricter rules like $K = 3$ and $K = 4$) to 0.4 dB (for the OR rule, $K = 1$). Even at a more stringent requirement of $P_D = 0.95$, the maximum observed loss remains bounded at around 0.5 dB for the $K = 1$ rule. This behavior is consistent with the theoretical expectation that the sample mean in CA-CFAR is the maximum likelihood estimator for exponential noise. However, as demonstrated in the subsequent sections, this minor homogeneous loss is a negligible price to pay for the significant immunity achieved against masking effects and false alarm surges in heterogeneous scenarios.

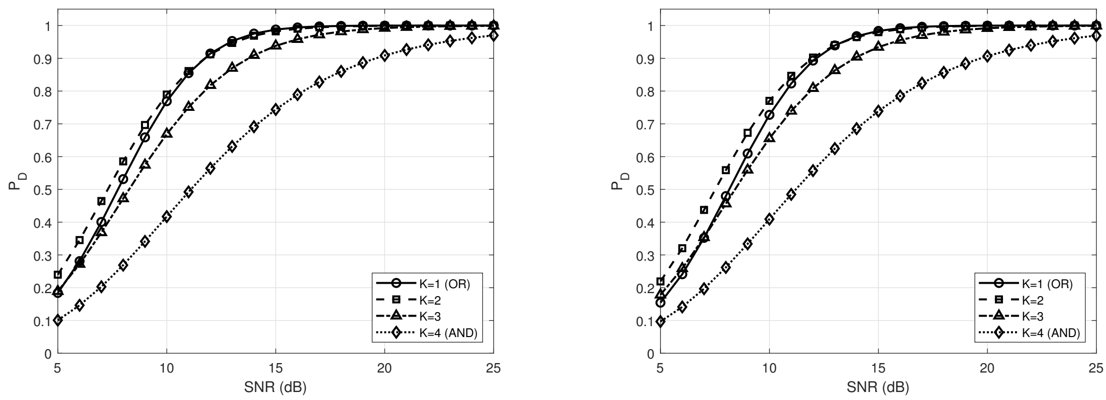

(a) (b)

Figure 3. The P_D versus SNR in a homogeneous environment: (a) CA-CFAR system and (b) OS-CFAR system

4.3. Robustness against multiple interfering targets

4.3.1. Impact of the number of interfered sensors (p)

We evaluate the system's resilience when $m = 4$ interfering targets interfere with p sensors. Figures 4(a) and 4(b) depicts P_D as a function of p (with SNR = INR = 15 dB). D-CA-CFAR (Figure 4(a)): the performance suffers catastrophic degradation. As p increases, the thresholds at interfered sensors drastically increase due to the averaging of high-power interference, effectively blinding those sensors ("masking effect"). Even with the robust "OR" rule ($K = 1$), when all sensors are affected, P_D drops below 0.5. D-OS-CFAR (Figure 4(b)): in stark contrast, regardless of p, the system maintains stable high performance ($P_D > 0.9$). This stability is physically explained by the sorting mechanism of OS-CFAR. Because the number of interfering targets ($m = 4$) is within the rejection capacity ($N - k = 4$), the k-th ordered sample remains representative of the noise floor. Consequently, the interference power does not inflated the local threshold, allowing the clean sensors to successfully drive the global K-out-of-L decision.

These results offer critical guidelines for operational radar networks. The analysis demonstrates that lower-K rules (e.g., $K = 1, 2$) act as a "survivability mode" in hostile environments. These rules require fewer sensors to declare a detection, allowing the global decision to be driven by the subset of sensors that remain unaffected by interference, effectively isolating the compromised nodes. This trend is fundamental to voting logic and generalizes to larger network sizes ($L > 4$), suggesting that distributed systems should prioritize "OR" or "majority" logic over "AND" logic when interference is detected.

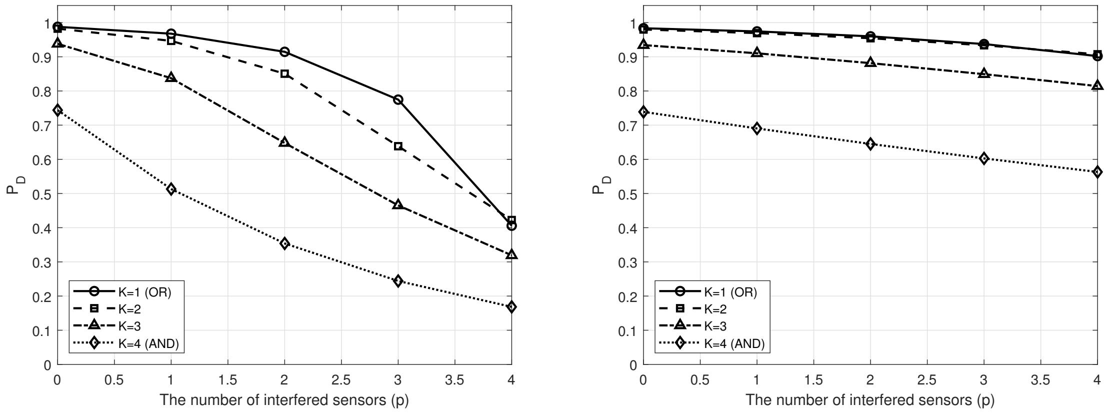

(a) (b)

Figure 4. The P_D versus the number of interfered sensors: (a) CA-CFAR system and (b) OS-CFAR system

4.3.2. Impact of interference power (INR)

Figures 5(a) and 5(b) investigates the sensitivity of the system to the interference power level, assuming $p = 2$ interfered sensors. D-CA-CFAR (Figure 5(a)): performance declines monotonically as INR increases. Stronger interference leads to deeper masking. D-OS-CFAR (Figure 5(b)): the performance curves are remarkably flat horizontal lines. This confirms the "interference immunity" property of the OS-CFAR. As long as the number of interferers is bounded, their power magnitude is irrelevant to the sorting-based estimation logic. Furthermore, the analysis confirms that lower majority rules offer superior robustness. This is because in a distributed network, a lower K requires fewer sensors to declare a detection. In a heterogeneous environment where some sensors are blinded by interference, a low-K rule effectively "ignores" the non-functioning sensors, relying on the remaining operational sensors to maintain global detection.

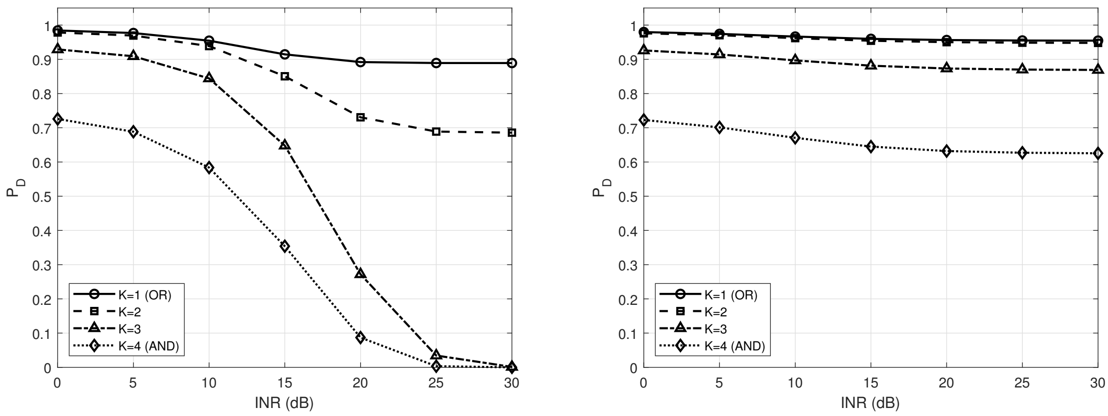

(a) (b)

Figure 5. The P_D versus INR of interfering targets: (a) CA-CFAR system and (b) OS-CFAR system

4.4. False alarm control at clutter edges

This section analyses the system's behavior during a transition from a clear region to a clutter region (CNR = 15 dB), assuming $p = 1$ sensor crosses the edge while $L - p = 3$ sensors remain in the clear region.

4.4.1. The "Surge" phenomenon

Figure 6 shows the global false alarm rate (P_F). Noise floor ($q \leq N/2$): when the CUT is in noise but clutter enters the window, both systems reduce P_F below the target 10^{-4} (masking). Interestingly, P_F does not drop to zero but converges to a "system noise floor" ($\approx 5 \times 10^{-5}$ for $K = 2$). This behavior is in contrast to conventional monostatic radars, where the false alarm probability decreases significantly as the clutter–edge position approaches ($N/2$) within the reference window. This property was verified by performing a much more accurate numerical analysis based on VPA, as described in section 3. This floor is maintained by the $L - p$ clean sensors, demonstrating the distributed architecture's inherent fault tolerance. False alarm surge ($q > N/2$): as shown in Figure 6(a), when the clutter edge crosses the CUT ($q > N/2$), the D-CA-CFAR experiences a severe false alarm surge, peaking at 6.2×10^{-4}. In contrast, D-OS-CFAR ($K = 2$) effectively suppresses this surge, limiting the peak to approximately 4.5×10^{-4}, which corresponds to a reduction of roughly 1.4 dB in equivalent power thresholding terms.

4.4.2. Sensitivity to clutter power (CNR)

Figure 6(b) shows the magnitude of the worst-case surge peak as a function of CNR. D-CA-CFAR: the peak height increases continuously with CNR, posing a severe risk of saturating the FC with false tracks in strong clutter environments. D-OS-CFAR: the surge peak exhibited a saturation behavior. This suggests that D-OS-CFAR provides a bounded "safety limit" for false alarms, making it a safer choice for dynamic environments with variable clutter power.

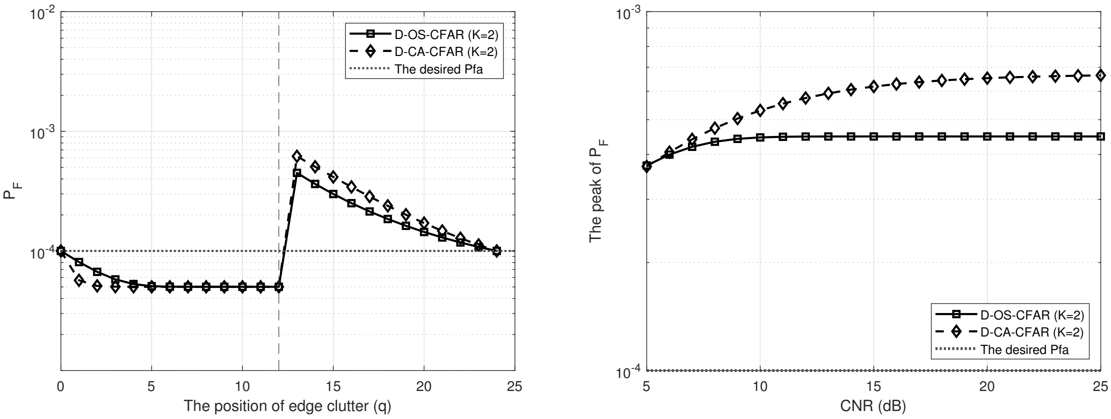

(a) (b)

Figure 6. The global false alarm rate (P_F) versus: (a) clutter edge position q and (b) CNR

5. CONCLUSION

This study established a rigorous performance benchmark for symmetric D-OS-CFAR systems based on the exact poisson binomial distribution and the VPA. The quantitative results demonstrate that the K-out-of-L scheme demonstrates improved robustness when K is optimally selected under moderate heterogeneity. While incurring a minor SNR loss of approximately 0.5 dB in homogeneous backgrounds, the D-OS-CFAR system maintains stable detection performance against masking effects and safely caps the false alarm surge at clutter edges to a manageable level. Furthermore, the analysis confirms that employing lower majority rules ($K \leq L/2$) is a critical survivability strategy. This highlights the practical importance of adaptive fusion threshold selection for maintaining stable operations in distributed radar and cognitive sensor networks. This analysis focused on CA and OS detectors, error-free channels, and identical sensors to ensure an exact closed form. Consequently, future research will extend this framework to other robust detectors, non-Gaussian clutter models, and dependent sensors while addressing practical constraints such as channel fading. Future work will focus on hardware validation with real radar data, adaptive K selection, and the integration of machine-learning-based threshold tuning to dynamically optimize performance in cognitive networks.

ACKNOWLEDGMENTS

The authors would like to thank the researchers and colleagues at the Department of Radar, Le Quy Don Technical University, for their valuable technical support and discussions. This research did not receive any specific research grant or contract from funding agencies in the public, commercial, or not-for-profit sectors.

FUNDING INFORMATION

Authors state no funding involved.

AUTHOR CONTRIBUTIONS STATEMENT

This journal uses the Contributor Roles Taxonomy (CRediT) to recognize individual author contributions, reduce authorship disputes, and facilitate collaboration.

Name of Author	C	M	So	Va	Fo	I	R	D	O	E	Vi	Su	P	Fu
Pham Van Hung	✓	✓	✓	✓	✓	✓		✓	✓	✓			✓	
Nguyen Dinh Tinh				✓		✓	✓			✓	✓	✓		✓

C	: **C**onceptualization	I	: **I**nvestigation	Vi	: **Vi**sualization
M	: **M**ethodology	R	: **R**esources	Su	: **Su**pervision
So	: **So**ftware	D	: **D**ata Curation	P	: **P**roject Administration
Va	: **Va**lidation	O	: Writing - **O**riginal Draft	Fu	: **Fu**nding Acquisition
Fo	: **Fo**rmal Analysis	E	: Writing - Review & **E**diting		

CONFLICT OF INTEREST STATEMENT

Authors state no conflict of interest.

INFORMED CONSENT

We have obtained informed consent from all individuals included in this study.

DATA AVAILABILITY

Data availability is not applicable to this paper as no new data were created or analyzed in this study.

REFERENCES

[1] J. C. García, L. A. Rivera, and J. Perez, "A Literature Review on Outlier Detection in Wireless Sensor Networks," *Journal of Advances in Information Technology*, vol. 15, no. 3, pp. 372–388, 2024, doi: 10.12720/jait.15.3.372-388.

[2] X. Zhou, X. Xu, W. Liang, Z. Zeng, and Z. Yan, "Deep-Learning-Enhanced Multitarget Detection for End-Edge-Cloud Surveillance in Smart IoT," *IEEE Internet of Things Journal*, vol. 8, no. 16, pp. 12588–12596, 2021, doi: 10.1109/JIOT.2021.3077449.

[3] L. Yan, S. Han, C. Hao, D. Orlando, and G. Ricci, "Innovative Cognitive Approaches for Joint Radar Clutter Classification and Multiple Target Detection in Heterogeneous Environments," *IEEE Transactions on Signal Processing*, vol. 71, pp. 1010–1022, 2023, doi: 10.1109/TSP.2023.3250084.

[4] B. K. Chalise, D. M. Wong, M. G. Amin, A. F. Martone, and B. H. Kirk, "Detection, Mode Selection, and Parameter Estimation in Distributed Radar Networks: Algorithms and Implementation Challenges," *IEEE Aerospace and Electronic Systems Magazine*, vol. 37, no. 11, pp. 4–22, 2022, doi: 10.1109/MAES.2022.3205568.

[5] W. Jiang, Y. Ren, Y. Liu, and J. Leng, "Artificial Neural Networks and Deep Learning Techniques Applied to Radar Target Detection: A Review," *Electronics*, vol. 11, no. 1, p. 156, 2022, doi: 10.3390/electronics11010156.

[6] M. A. Richards, Fundamentals of Radar Signal Processing, 3rd ed., vol. 58, no. 12. McGraw-Hill Education, 2014.

[7] M. A. Richards, J. A. Scheer, and W. A. Holm, Principles of modern radar: Basic principles, 2nd ed., vol. 1. SciTech Publishing / The Institution of Engineering and Technology, 2010, doi: 10.1049/sbra021e.

[8] H. M. Finn and R. S. Johnson, "Adaptive detection mode with threshold control as a function of spatially sampled clutter level estimates," *RCA Review*, vol. 29, no. 3, pp. 414–464, 1968.

[9] M. Y. Rihan, Z. B. Nossair, and R. I. Mubarak, "An improved CFAR algorithm for multiple environmental conditions," *Signal, Image and Video Processing*, vol. 18, no. 4, pp. 3383–3393, 2024, doi: 10.1007/s11760-024-03001-x.

[10] P. P. Gandhi and S. A. Kassam, "Analysis of CFAR Processors in Nonhomogeneous Background," *IEEE Transactions on Aerospace and Electronic Systems*, vol. 24, no. 4, pp. 427–445, 1988, doi: 10.1109/7.7185.

[11] H. Rohling, "Radar CFAR Thresholding in Clutter and Multiple Target Situations," *IEEE Transactions on Aerospace and Electronic Systems*, vol. AES-19, no. 4, pp. 608–621, 1983, doi: 10.1109/TAES.1983.309350.

[12] Z. Wang and J. Wang, "An improved CFAR algorithm based on maximum selection and ordered statistics," in *IMCEC 2024 - IEEE 6th Advanced Information Management, Communicates, Electronic and Automation Control Conference*, 2024, pp. 1459–1462, doi: 10.1109/IMCEC59810.2024.10575521.

[13] V. Kanawade, C. Ganguly, M. K. Manoj, and J. Valarmathi, "Comparison of CFAR Algorithms in Real Time Target Detection and Tracking using Millimeter Wave Radar," in *2025 IEEE International Conference on Interdisciplinary Approaches in Technology and Management for Social Innovation, IATMSI 2025*, 2025, pp. 1–5, doi: 10.1109/IATMSI64286.2025.10985433.

[14] F. Yavuz, "Radar Target Detection with CNN," in *2021 29th European Signal Processing Conference (EUSIPCO)*, 2021, pp. 1581–1585, doi: 10.23919/EUSIPCO54536.2021.9616316.

[15] B. Zhang, J. Zhou, J. Xie, and W. Zhou, "Weighted likelihood CFAR detection for Weibull background," *Digital Signal Processing: A Review Journal*, vol. 115, p. 103079, 2021, doi: 10.1016/j.dsp.2021.103079.

[16] H. E. Bouchelaghem, M. Hamadouche, F. Soltani, and K. Baddari, "Distributed Clutter-Map Constant False Alarm Rate Detection Using Fuzzy Fusion Rules," *Radioelectronics and Communications Systems*, vol. 62, no. 1, pp. 1–5, 2019, doi: 10.3103/S0735272719010011.

[17] M. Rane, V. Bendre, and R. Sor, "An Overview of Design and Implementation of Various Ordered Statistical Methods for Target Detection in RADAR," in *2023 7th International Conference On Computing, Communication, Control And Automation, ICCUBEA*, 2023, pp. 1–6, doi: 10.1109/ICCUBEA58933.2023.10392110.

[18] T. Jeong, S. Park, J. W. Kim, and J. W. Yu, "Robust CFAR Detector With Ordered Statistic of Sub-Reference Cells in Multiple Target Situations," *IEEE Access*, vol. 10, pp. 42750–42761, 2022, doi: 10.1109/ACCESS.2022.3168707.

[19] C. Guillén, N. Chávez, and J. Bacallao, "Radar detection in the moments space with constant false alarm rate," *Digital Signal Processing*, vol. 114, p. 103080, 2021, doi: 10.1016/j.dsp.2021.103080.

[20] S. Gong, W. Long, D. Ben, and M. Pan, "Adaptive fuzzy CFAR detection fusion algorithm for netted radar," *Systems Engineering and Electronics*, vol. 44, no. 1, pp. 100–107, 2022, doi: 10.12305/j.issn.1001-506X.2022.01.14.

[21] T. Diskin, Y. Beer, U. Okun, and A. Wiesel, "CFARnet: Deep learning for target detection with constant false alarm rate," *Signal Processing*, vol. 223, p. 109543, 2024, doi: 10.1016/j.sigpro.2024.109543.

[22] C. Xiu and Y. Li, "Adaptive Constant False Alarm Rate Detector Based on Long Short-term Memory Network," *Radioengineering*, vol. 34, no. 1, pp. 132–142, 2025, doi: 10.13164/RE.2025.0132.

[23] Z. Chair and P. K. Varshney, "Optimal Data Fusion in Multiple Sensor Detection Systems," *IEEE Transactions on Aerospace and Electronic Systems*, vol. AES-22, no. 1, pp. 98–101, 1986, doi: 10.1109/TAES.1986.310699.

[24] M. Barkat and P. K. Varshney, "Decentralized CFAR signal detection," *IEEE Transactions on Aerospace and Electronic Systems*, vol. 25, no. 2, pp. 141–149, 1989, doi: 10.1109/7.18676.

[25] M. K. Uner and P. K. Varshney, "Distributed cfar detection in homogeneous and nonhomogeneous backgrounds," *IEEE Transactions on Aerospace and Electronic Systems*, vol. 32, no. 1, pp. 84–97, 1996, doi: 10.1109/7.481251.

[26] P. Z. Liu, R. Y. Pan, and G. F. Guo, "Parameter optimization of decentralized OS-CFAR system based modified PSO method," *Advanced Materials Research*, 532–533, pp. 881–886, Jun. 2012, doi: 10.4028/www.scientific.net/amr.532-533.881.

[27] A. Gouri, A. Mezache, and H. Oudira, "Distributed CA-CFAR and OS-CFAR Detectors Mentored by Biogeography Based Optimization Tool," *International Journal of Information Science and Technology*, vol. 3, no. 3, pp. 20–29, 2019, doi: 10.57675/IMIST.PRSM/IJIST-V3I3.60.

[28] M. A. Bouteldja, M. Baadeche, and F. Soltani, "Optimization of Distributed Mean-Level CFAR Detectors Using GA and PSO Algorithms," *Lecture Notes in Networks and Systems*, pp. 88–99, 2021, doi: 10.1007/978-3-030-92038-8_9.

[29] V. H. Pham, T. H. Nguyen, D. M. Nguyen, and H. Morishita, "A New Method Based on Copula Theory for Evaluating Detection Performance of Distributed-Processing Multistatic Radar System," *IEICE Transactions on Communications*, vol. E105–B, no. 1, pp. 67–75, 2022, doi: 10.1587/transcom.2021EBP3001.

[30] V. H. Pham, T. H. Nguyen, and H. Morishita, "Detection Performance Analysis of Distributed-Processing Multistatic Radar System with Different Multivariate Dependence Models in Local Decisions," *IEICE Transactions on Communications*, vol. E105B, no. 9, pp. 1097–1104, 2022, doi: 10.1587/transcom.2021EBP3184.

[31] B. K. Chalise and K. T. Wagner, "Distributed GLRT-based Detection of Target in SIRP Clutter and Noise," in *IEEE National Radar Conference - Proceedings*, 2021, pp. 1–6, doi: 10.1109/RadarConf2147009.2021.9455177.

[32] X. Mao *et al.*, "A Model Fusion Distributed Kalman Filter for Non-Gaussian Measurement Noise," *IEEE Internet of Things Journal*, vol. 12, no. 10, pp. 14677–14690, 2025, doi: 10.1109/JIOT.2025.3526240.

[33] Z. Yang, X. Li, C. Yuan, and J. Sun, "A Distributed OS-CFAR Detection Method Under Log-Normal Clutter," in *2025 18th International Congress on Image and Signal Processing, BioMedical Engineering and Informatics (CISP-BMEI)*, 2025, pp. 1–5, doi: 10.1109/CISP-BMEI68103.2025.11259384.

[34] L. J. Gleser, "On the Distribution of the Number of Successes in Independent Trials," *The Annals of Probability*, vol. 3, no. 1, pp. 295–312, 2007, doi: 10.1214/aop/1176996461.

[35] The MathWorks Inc., "MATLAB and Symbolic Math Toolbox," Massachusetts, United States, 2024.

[36] N. J. Higham, "Accuracy and stability of numerical algorithms," *Society for Industrial and Applied Mathematics*, vol. 94. 2002, doi: 10.1137/1.9780898718027.

BIOGRAPHIES OF AUTHORS

Pham Van Hung received the B.S. degree in Electrical and Electronic Engineering in 2011, and the M.S. and Ph.D. degrees in Radar and Navigation Engineering from Le Quy Don Technical University (LQDTU), Vietnam, in 2016 and 2024, respectively. He is currently working as a lecturer at LQDTU. His research interests include detection theories, radar clutter, multi-static radar systems, signal and data processing for radar systems, and data fusion. In this current study, his major contributions involved the conceptualization of the distributed CFAR model, the derivation of the exact mathematical framework, and performing the numerical simulations. He can be contacted at email: hungpv_k31@lqdtu.edu.vn.

Nguyen Dinh Tinh received the B.E. degree in Electronics-Telecommunications in 2008, and the M.E. and Ph.D. degrees in Radar and Navigation Engineering from Le Quy Don Technical University (LQDTU), Vietnam, in 2012 and 2023, respectively. He is currently working as a lecturer and researcher at LQDTU. His research interests encompass antenna theories, signal processing for radar systems, synthetic aperture radar (SAR), and sonar. In this study, he contributed to the supervision of the research project, the validation of the analytical results, and the reviewing and editing of the manuscript. He can be contacted at email: tinhnd_k31@lqdtu.edu.vn.